The dusty AGB star RS CrB: first mid-infrared interferometric observations with the Keck Telescopes

B. Mennesson[1], C. Koresko[2], M.J. Creech-Eakman[3], E. Serabyn[1], M.M. Colavita [1], R. Akeson[2], E. Appleby[4], J. Bell[4], A. Booth[1], S. Crawford[1], W. Dahl[4], J. Fanson[1], C. Felizardo [2], J. Garcia[1], J. Gathright[4], J. Herstein[2], E. Hovland[1], M. Hrynevych[4], E. Johansson[4], D. Le Mignant[4], R. Ligon[1], R. Millan-Gabet[2], J. Moore [1], C. Neyman[4], D. Palmer[1], T. Panteleeva[4], C. Paine[1], S. Ragland[4], L. Reder[1], A. Rudeen[4], T. Saloga [4], M. Shao[1], R. Smythe[1], K. Summers [4], M. Swain[1], K. Tsubota[4], C. Tyau[4], G. Vasisht[1], P. Wizinowich [4], J. Woillez[4]

ABSTRACT

We report interferometric observations of the semi-regular variable star RS CrB, a red giant with strong silicate emission features. The data were among the first long baseline mid-infrared stellar fringes obtained between the Keck telescopes, using parts of the new nulling beam combiner. The light was dispersed by a low-resolution spectrometer, allowing simultaneous measurement of the source visibility and intensity spectra from 8–12 μm. The interferometric observations allow a non-ambiguous determination of the dust shell spatial scale and relative flux contribution. Using a simple spherically-symmetric model, in which a geometrically thin shell surrounds the stellar photosphere, we find that $\sim$ 30% to $\sim$ 70% of the overall mid-infrared flux - depending on the wavelength - originates from 7-8 stellar radii. The derived shell opacity profile shows a broad peak around 11 microns ($\tau \simeq 0.06$), characteristic of Mg-rich silicate dust particles.

Subject headings: instrumentation: interferometers —infrared: stars — stars: late type — stars: individual (RS CrB)

[1]Jet Propulsion Laboratory, California Institute of Technology, 4800 Oak Grove Drive, Pasadena CA 91109-8099

[2]Michelson Science Center, California Institute of Technology, 770 South Wilson Avenue, Pasadena CA 91125

[3]New Mexico Tech, Dept of Physics, 801 Leroy Place, Socorro, NM 87801

[4]W.M. Keck Observatory, California Association for Research in Astronomy, 65-1120 Mamalahoa Highway, Kamuela, HI 96743

1. Introduction

The apparent interferometric sizes of variable red giants vary dramatically - up to a factor of 3 - with wavelength and pulsation phase (Tuthill, Haniff, & Baldwin 1995; Tuthill, Monnier, & Danchi 2000; Weiner et al. 2000; Mennesson et al. 2002) (Thompson, Creech-Eakman, & van Belle 2002; Perrin et al. 2004; Weiner et al. 2004). These large variations challenge current hydrodynamical and line opacity models of these stars, indicating that their extended atmospheres are extremely complex. Simultaneous spectroscopic and high angular resolution observations over a wide wavelength range are key to understanding the various phenomena these stars exhibit, including photometric pulsation, high mass-loss rates, dust nucleation, and formation of molecular layers and masers. High angular resolution thermal infrared observations of bright red giants in *narrow bandpasses* ($\Delta\lambda/\lambda \simeq 10^{-4} - 10^{-3}$) have been available for some time (Danchi et al. 1994). The Keck Interferometer Nuller (KIN) (Serabyn et al. 2004) and the MIDI instrument on the VLTI (Leinert et al. 2003) offer much greater spectral coverage, typically over the whole 8–13 μm region, with a sensitivity goal of about 1 Jy.

The Keck Interferometer is nearly ideal for the study of such stars. Its 85 m baseline produces a fringe spacing of 27 mas at 11 μm, commensurate with the expected angular scales of most variable red giants located within 1 kpc (photosphere diameter of a few mas, with thermal emission from dust peaking within several stellar radii). The detection is carried out by means of a low-resolution spectrometer ($\lambda/\Delta\lambda \simeq 35$), sensitive across a bandpass which spans the broad opacity peaks characteristic of various types of O-rich and C-rich dusts.

RS CrB was the first star successfully observed with the Keck Interferometer's mid-infrared (MIR) beam combiner. It is a bright semi-regular variable of type *a*, quite similar to a Mira but with smaller photometric variations ($\Delta m_V \simeq$ 1-2). It has a mean pulsation period of 332 days (Kholopov et al. 1992) and is classified as a red giant of spectral type M7, with a 12 μm flux of 53 Jy (Beichman et al. 1988). It has an oxygen-rich dust shell with strong silicate emission features detected by the IRAS Low Resolution Spectrometer (LRS) (class SE6t, (Sloan & Price 1998)). Ita et al. (2001) detected SiO maser emission around RS CrB, which can be regarded as a tracer of dense molecular gas in the inner region ($\simeq$ 2 stellar radii) of the circumstellar envelope (e.g. VLBA images of TX Cam (Diamond and Kemball 1999) and other Miras (Cotton et al. 2004)).

We present a measurement of the wavelength-dependent fringe visibility of RS CrB from 8–12 μm, a spectral region where both the central star and its surrounding dust shell are visible. In combination with the intensity spectrum measured across the same band with the individual Keck telescopes, it is possible to determine the relative brightness of the two components, the spatial extent of the shell, and its opacity spectrum.

2. Observations

The observations were made on August 8 2004, using a subset of the KIN optics (Mennesson et al. 2003; Serabyn et al. 2004) as a two-input beam combiner, without most of the special features needed to produce the high fringe contrast (> 0.99) required for nulling. The telescopes each fed one of the two inputs of the primary modified Mach- Zehnder (MMZ) symmetric beam combiner (Serabyn & Colavita 2001). One of the two resulting outputs was sent to KALI, a low-resolution MIR spectrometer (Creech-Eakman et al. 2003). KALI uses a Boeing Si:As BIB detector, cooled to 4 K, with the optics and radiation shield cooled to ~ 90 K using LN_2. A cold internal pinhole (equivalent diameter $2\lambda/D$) at an intermediate focus provides spatial filtering. Direct-view prisms disperse the N-band light into 14 spectral channels. The central wavelengths for the channels were measured using Fourier Transform Spectroscopy (FTS) scans of a hot filament. They ranged from 8.16–12.01 μm, with the channel width varying from $\simeq 0.2$ μm on the red end to $\simeq 0.4$ μm on the blue end.

RS CrB was observed at a single, quasi constant projected baseline (80.6– 80.9 m), along with a set of calibrator stars (early K giants) with known near-infrared (NIR) diameters. To allow for the differential limb darkening between the NIR and MIR wavelengths, we adopted conservative error bars on the estimated calibrators diameters in the MIR. A list of the stars and their properties is given in Table 1. The observation sequences were similar to those used at NIR wavelengths for the Keck interferometer (Colavita et al. 2003). The fringe amplitude was measured accurately through a fast (40 Hz) optical path difference modulation. Each star was visited between 3 and 4 times, with typically one or two minutes spent tracking the fringe during a visit.

The most important source of uncertainty in these visibility measurements was the removal of the strong and variable thermal background. For each of the two beams, the absolute stellar signal was determined through sky chopping. A spatial chop was implemented using the fast tip-tilt mirrors of the Keck adaptive optics systems (Wizinowich et al. 2003) at a frequency of 5 Hz. Because of beamwalk on the optics upstream of the tip-tilt mirror, a fraction of the thermal background is also modulated. To correct for this bias, the demodulated background signal was determined through a similar chopping measurement on blank sky. After this calibration, stellar signals derived from the various single aperture observations still exhibited fluctuations at the $\simeq$ 5-10% level, which we hope to overcome in the future with a symmetric three position chop. This is currently the main contributor to the visibility error bars, both on RS CrB and the calibrators. The data reduction was otherwise similar to that used for NIR visibility measurements at PTI and KI (Colavita et al. 1999). The calibrator observations were used to measure the "system visibility" (the response of the interferometer to a point-source), which did not show any significant time dependence.

Its value during the RS CrB observations was estimated by combining the system visibilities measured on all three calibrators (Table 1). The resulting calibrated visibility curve for RS CrB is plotted in Fig 1, showing that the source is clearly resolved.

3. Modeling and interpretation

Since all measurements presented here were obtained with a single baseline orientation, only models with spherical symmetry are considered. There is also astrophysical justification for this choice, both on a theoretical and observational basis. The envelope surrounding an AGB star can be described to first order by a spherically symmetric outflow at a constant velocity of $\sim$ 10 km/sec, in which the material is heated by friction between gas and dust particles and cooled primarily by the line radiation of molecules such as H_2O (Habing 1996). Also, maser observations of *single* evolved stars generally show ring-like structures which are much more compatible with spherical geometries than disk-like ones (Diamond and Kemball 1999; Cotton et al. 2004). Finally, recent NIR interferometric phase closure measurements failed to detect asymmetric structures in a sample of 10 M-class semi-regular variables (S. Ragland, priv. comm.).

We do not expect single component brightness distributions to accurately describe dusty red giants in the MIR. Yet, a uniform disk fit allows a simple representation of the visibility data at each wavelength, and we use it here as a convenient starting point. The resulting apparent diameter, plotted in Fig. 2, increases rapidly between 8.2 and 10 μm and reaches a plateau at longer wavelengths. The apparent size and its chromatic variations are large, pointing to a variable opacity effect in the upper atmosphere, rather than to true changes in the physical dimension of a single photosphere. Adopting now a two component representation, consisting of a central photosphere surrounded by a dust shell with a variable opacity, the visibility is sensitive to the size of the shell and its brightness relative to the central star, and depends only weakly on the size of the stellar photosphere. A straightforward interpretation to the apparent size variations in Fig. 2 is that the relative brightness of the shell increases with wavelength across the measured band, becoming dominant at the long wavelengths. This behavior correlates nicely with the SE6 classification of RS CrB in the silicate dust sequence (Sloan & Price 1998), which shows a similar variation of the infrared excess versus wavelength.

We now model the shell as infinitely thin, with angular diameter Φ_{shell}, optical depth $\tau(\lambda)$ and temperature T_{shell}, surrounding a blackbody photosphere of angular diameter Φ_* and temperature T_*. This model is similar to the one previously applied to molecular layers around red giants (Perrin et al. 2004; Scholz 2001). It predicts both the visibility spectrum

and the intensity spectrum across the observed bandpass. We explored a grid of model parameters $\{T_*, \Phi_*, T_{shell}, \Phi_{shell}\}$, computing $\chi 2$ per spectral channel for the visibility at each point in the grid. The spectrum of RS CrB derived from our single Keck telescope observations (Fig. 3) is used to determine $\tau(\lambda)$ at each point. We constrain the stellar temperature T_* to be 3100 ± 150 K, corresponding to the range of effective temperatures proposed for M7 giants (Dyck et al. 1996; Perrin et al. 1998). The value of Φ_* can be estimated from a blackbody fit to the NIR flux (Kerschbaum and Hron 1994). The results range from 3.7–4.2 mas between the J and M bands. This estimate is likely crude, however, as it neglects the effect of the circumstellar envelope. In light of this uncertainty, we allowed Φ_* to range from 2.5–5 mas. The shell diameter was allowed to vary between 1 and 50 times Φ_*, while the maximum shell temperature was set to 1500 K, a reasonable upper limit for the grain sublimation temperature. The error bar on each parameter is computed as the deviation that increases the χ^2 by one after reoptimizing all the other parameters. The resulting values are: $\Phi_* = 3.78 \pm 0.20$ mas, $\Phi_{shell} = 27.6 \pm 1.2$ mas, $T_{shell} = 1160 \pm 300$ K, and $\tau_{max} = \tau_{11.1\mu m}$ = 0.04-0.3. The agreement between the model and the observed V^2 is excellent (χ^2 per point = 0.38, Fig. 1, plain curve) showing that the visibility data at all wavelengths can be reproduced by a 2-component model with a fixed, *wavelength independent* geometry, and an opacity profile fixed by the observed intensity spectrum.

The shell diameter Φ_{shell} is the most accurately constrained parameter. It indicates that most of the flux at long wavelengths - probing the dust emission zone- originates from a region located around 7-8 stellar radii. Interestingly, this is comparable to the inner dust shell size derived by the MIDI instrument for the Mira star RR Sco (Ohnaka et al. 2005). For wavelengths shorter than 10 μm, the contribution from the central star is visible and well constrained by the observed V^2. For the stellar temperature range adopted, the fit yields a central object diameter consistent with the NIR photometry. We expect the photospheric diameter as measured at shorter NIR wavelengths to be smaller, due to the effect of molecular layers around this type of star (Hinkle & Barnes 1979; Tsuji 1988; Yamamura et al. 1999) which is more prominent at long infrared wavelengths (Mennesson et al. 2002; Weiner et al. 2004). This has now been confirmed by IOTA interferometric observations at 1.65μm - a region free of significant molecular absorption -, which yield an uniform disk diameter of 3.15 ± 0.12 mas for RSCrB (John Monnier, priv. comm., June 2005).

The model fit depends on the overall flux from the shell rather than on T_{shell} and $\tau(\lambda)$ individually, so those parameters are not separately well constrained by the fit. T_{shell} must be at least ~ 850 K to account for the observed shell flux at the shortest wavelengths, and is presumably below ~ 1450 K, as that is the maximum radiative equilibrium temperature allowing silicate grains to survive in a stationary flow around a typical mass-losing AGB star (Willson 2000). Within this temperature range, the corresponding $\tau(\lambda)$ varies over

almost an order of magnitude. Although the overall dust opacity is not well constrained, its *shape* is (Fig. 4). The sharp opacity rise observed between 8 and 9.7 μm is characteristic of amorphous silicates. The shoulder seen near 11 μm is often seen in low mass-loss rate AGB stars (Waters et al. 1998) and may indicate the presence of another solid, such as amorphous alumina. It could for instance be in the form of Mg-Fe aluminosilicate compounds (Mutschke et al. 1998). Alternatively, this 11 μm feature could reflect the presence of Mg-rich crystalline forms of olivine such as forsterite (Mg_2SiO_4), which exhibits an absorption peak around 11.2μm (Koike et al. 2003). Our spectral resolution does not allow to choose between these two different scenarios at present.

4. Conclusions

Using broad-band thermal interferometry with the twin Keck telescopes, we have measured the size and opacity profile of the dust shell around RS CrB, an AGB star with strong silicate emission features. The dust shell "radius" derived in our model can be understood as a characteristic size of the weighted brightness distribution of the shell. Strikingly, a single shell radius value of 7-8 R_* allows to fit the data over the whole 8-12 microns range, suggesting that most of the detected emission arises from dust in this region. The opacity profile which fits both the intensity and visibility spectra indicates the presence of amorphous silicates, and possibly other dust species like amorphous alumina or Mg-rich olivine in this region. The V^2 measurements obtained at the blue end of our bandpass, where the dust opacity is low, constrain the size and fractional amount of flux coming from the "central" star. These first results obtained with the Keck Interferometer already demonstrate the value of wide band long baseline thermal infrared interferometry. Interferometric observations allow non ambiguous determination of the spatial brightness distribution very close to the central source, information that cannot be derived from spectroscopy alone. Finally, the wide spectral coverage provides access to different physical regimes and can be used to simultaneously constrain multiple components of an astronomical source.

The Keck Interferometer is funded by the National Aeronautics and Space Administration (NASA). Part of this work was performed at the Jet Propulsion Laboratory, California Institute of Technology, and at the Michelson Science Center (MSC), under contract with NASA. The Keck Observatory was made possible through the generous financial support of the W.M. Keck Foundation. Finally, the authors wish to recognize and acknowledge the very significant cultural role and reverence that the summit of Mauna Kea has always had within the indigenous Hawaiian community. We are most fortunate to have the ability to conduct observations from this mountain.

REFERENCES

Beichman C.A. et al., IRAS catalogs and Atlases, Version 2, Explanatory Supplement, NASA Publication 1190, I.

Beichman C.A., Woolf, N.J. and Lindensmith C.A., 1999, The Terrestrial Planet Finder: a NASA Origins Program to Search for Habitable Planets, JPL Publication 99-3.

Colavita, M.M. et al. 1999, ApJ 510, 505

Colavita M.M. et al. 2003, ApJ, 592, 83

Cotton W. et al. 2004, A&A, 414, 275

Creech-Eakman M.J. et al. 2003, in SPIE Conf. Proceedings 4841, 330

Danchi W. et al. 1994, AJ, 107, 1469

Diamond P.J. & Kemball A.J. 1999, IAU Symposium 191, edited by T. Le Bertre, A. Lebre and C. Waelkens, 195

Dyck H.M. et al. 1996, 111, 1705

Fogel M.E. & Leung C.M. 1998, ApJ, 501, 175.

Habing H.J. 1996, A&A Rev. 7, 2, 97

Hinkle K.H. & Barnes T.G. 1979, ApJ, 227, 923

Ita Y. et al. 2001, A&A, 376, 112

Kerschbaum F. & Hron J. 1994, A&AS, 106, 397

Kholopov et al. 1992, Bulletin d'Information Centre Donnees Stellaires, Vol 40, 15

Koike C. et al. 2003, A&A 399, 1101

Koresko C.D., Mennesson B.P. , Serabyn E., Colavita M., Akeson R., Swain M. 2003, SPIE 4838, 625

Leinert C. et al. 2003, Astrophysics & Space Science, 286, 1, 73

Mennesson B. et al. 2002, ApJ, 579, 446

Mennesson B. et al. 2003, in Conf. Towards Other Earths: DARWIN/TPF and the Search for Extrasolar Terrestrial Planets, ed. M. Fridlund & T. Henning, (Noordwijk: ESA-SP-539), 525.

Monnier J. et al. 2004, ApJ, 605, 436

Mutschke H. et al. 1998, A&A 333, 188

Ohnaka K. et al 2005, A&A, 429, 1057

Perrin G. et al. 1998, A&A, 331, 619

Perrin G. et al. 2004, A&A, 426, 279

Scholz M. 2001, MNRAS, 321, 347

Serabyn E. and Colavita M. M. 2001, Applied Optics, 40, 1668

Serabyn E. et al. 2004, SPIE Conf. Ser. 5491, 806, ed. W.A. Traub

Sloan G.C. & Price S.D. 1998, ApJS, 119, 141

Thompson R.R., Creech-Eakman M.J. & van Belle G.T. 2002, ApJ, 124, 1706

Tsuji T. 1988, A&A, 197, 185

Tuthill, P.G., Haniff, C.A. & Baldwin, J.E., 1995, MNRAS, 277, 1541

Tuthill, P.G., Monnier, J.D. & Danchi, W.C., 2000, SPIE Conf. Ser. 4006, 491, , ed. P.J. Léna & A. Quirrenbach

Waters R. et al. 1998, A&A, 331, L61

Weiner J. et al. 2000, ApJ, 544, 1097

Weiner J. 2004, ApJ, 611, 37

Willson L.A. 2000, ARA&A, 38, 573

Wizinowich P. et al. 2003, SPIE Proc. 4839, 9

Yamamura, I., de Jong T.,& Cami J., 1999, A&A, 348, L55

Table 1. Target and Calibrator Stars

Star	Type	θ_* (mas)	Fringe Time (sec)	$V2_{sys}$
RS CrB	M7 SRa	$\sim$4	411	
ϵ CrB	K2III	2.81 ± 0.1 [a]	676	0.57 ± 0.15
39 Cyg	K3III	2.82 ± 0.1 [a]	604	0.67 ± 0.11
ϵ Cyg	K0III	4.47 ± 0.2 [a,b]	598	0.71 ± 0.08

Note. — For RS CrB, the quoted diameter is the one expected from near infrared photometry, assuming a spherical blackbody at 3100 K. The calibrator diameter values are taken from (a): the CHARM Catalog (Richichi et al. 2005), and (b): the Catalog of LBSI Calibrator Stars (Borde et al. 2002). The $V2_{sys}$ for each calibrator is an average of the values over the bandpass and over visits to the star.

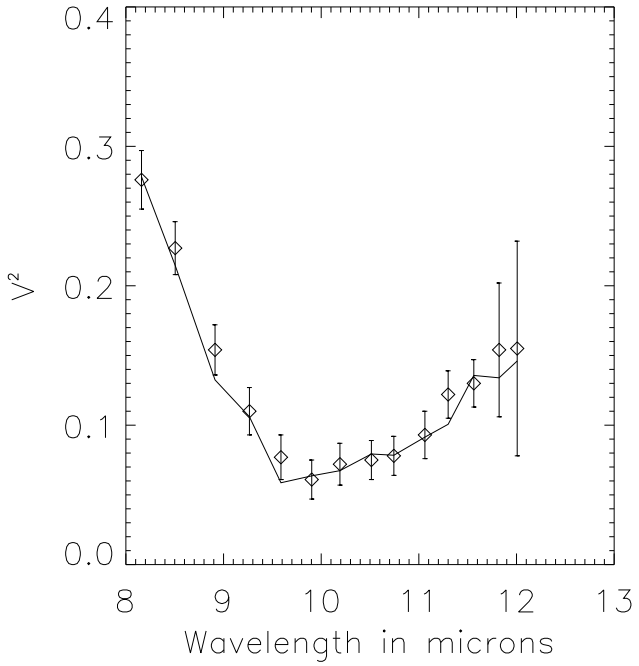

Fig. 1.— Diamonds and error bars (1-σ): observed visibility spectrum for RS CrB. Plain curve: best model fit.

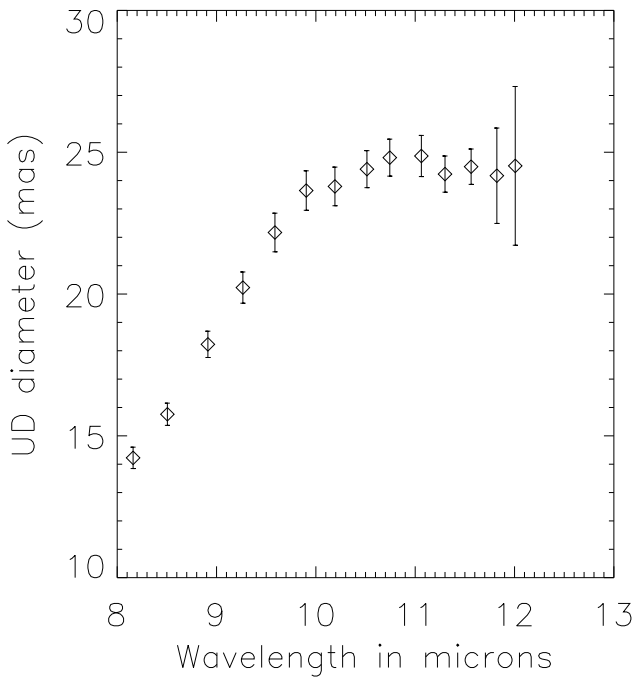

Fig. 2.— Uniform disk diameters obtained when fitting the observed V^2 at each wavelength.

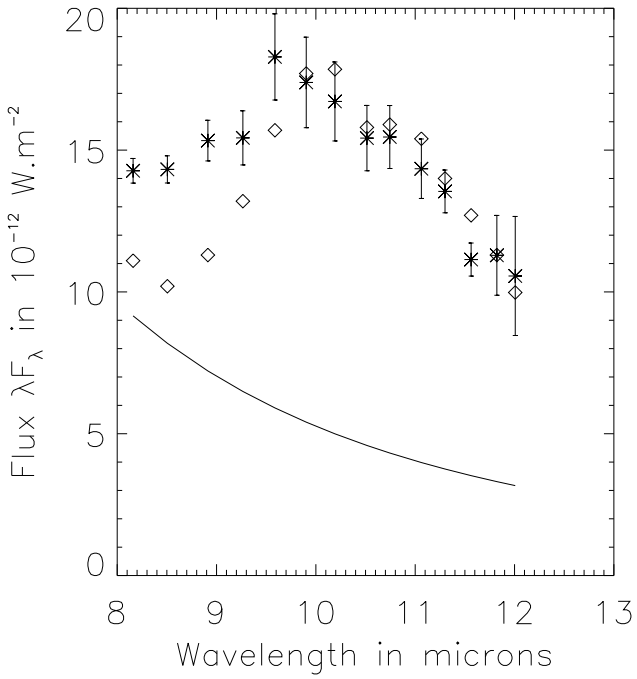

Fig. 3.— RS CrB spectra. Crosses and error bars: observed spectrum using the individual Keck telescopes. The raw spectrum was normalized by the KALI responsivity, which is determined by comparing raw KALI spectra of the calibrator stars with their IRAS LRS spectra. Diamonds: IRAS LRS spectrum converted to KIN's spectral resolution. The Keck measured spectrum has an overall flux close to that measured two decades earlier by IRAS, but shows significantly more flux at the blue end. Plain curve: naked star spectrum, for the best V^2 fit parameters.

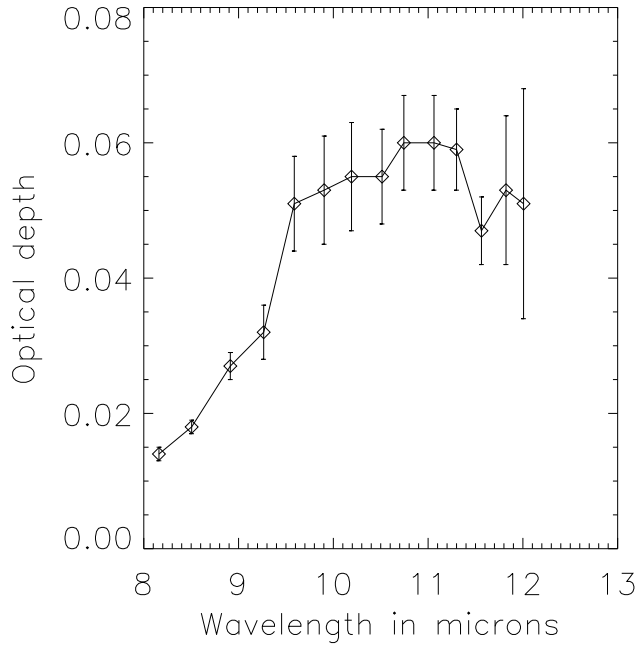

Fig. 4.— Optical depth profile derived from the single telescope spectra, using the best model parameters: $\Phi_* = 3.78\,\mathrm{mas}$, $T_* = 3100\,\mathrm{K}$, $\Phi_{shell} = 27.6\,\mathrm{mas}$ and $T_{shell} = 1160\,\mathrm{K}$.